

# High Resolution CCD Polarization Imaging Sensor

Viktor Gruev and Tim York  
Computer Science and Engineering Department  
Washington University in St. Louis  
St. Louis, MO 63130, USA  
vgruev@wustl.edu

**Abstract**—We present a novel polarization imaging sensor by monolithically integrating aluminum nanowire optical filters with an array of CCD imaging elements. The CCD polarization image sensor is composed of 1000 by 1000 imaging elements with 7.4 $\mu$ m pixel pitch. The image sensor has a dynamic range of 65dB and signal-to-noise ratio of 45dB. The CCD array is covered with an array of pixel-pitch matched nanowire polarization filters with four different orientations offset by 45°. The complete imaging sensor is used for real-time reconstruction of the shape of various objects.

## INTRODUCTION

Traditional CMOS and CCD imaging sensors capture two of the three fundamental properties of light: color and intensity [1]. The third fundamental property of light, polarization, has been largely ignored by the imaging industry and research community in part by the human inability to “see” polarization properties [2]. Nevertheless polarization-contrast imaging has proven to be very useful in gaining additional visual information in optically scattering environments, such as target contrast enhancement in hazy/foggy conditions [3], depth map of the scene in underwater imaging [4], and in normal environmental conditions, such as non-contact fingerprint detection [5] among others. Polarization imaging tends to provide information that is largely uncorrelated with spectral and intensity images.

In order to capture the optical properties of partially polarized light, three parameters are of importance: the intensity of the wave, the angle of polarization (AoP) and the degree of linear polarization (DoLP). There are different ways of computing DoLP and AoP of the electric-field vector, one of which is presented by equation (1) and (2).

$$DoLP = \frac{\sqrt{S_1^2 + S_2^2}}{S_0} \quad (1)$$

$$AoP = \frac{1}{2} \arctan\left(\frac{S_2}{S_1}\right) \quad (2)$$

In equation (1) and (2),  $S_0$ ,  $S_1$  and  $S_2$  are known as the Stokes parameters and are defined by equations (3) through (5):

$$S_0 = I(0^\circ) + I(90^\circ) \quad (3)$$

$$S_1 = I(0^\circ) - I(90^\circ) \quad (4)$$

$$S_2 = I(45^\circ) - I(135^\circ) \quad (5)$$

In equations (3) through (5),  $I(0^\circ)$  is the intensity of the e-vector filtered with a 0 degree linear polarization filter;  $I(45^\circ)$  is the intensity of the e-vector filtered with a 45 degree linear polarization filter and so on. In order to compute the first three Stokes parameters, the incoming light wave must be filtered with four linear polarization filters offset by 45°. Hence, an imaging sensor capable of characterizing partially polarized light has to employ four linear polarization filters offset by 45° together with an array of imaging elements.

Recovering polarization information in the visible spectrum has typically been implemented using standard CMOS or CCD imaging sensors coupled with electrically controlled polarization filter [6]. These imaging systems, known as division of time polarimeters, filter the imaged environment with four time multiplexed polarization filters offset by 45°, record the total intensity of the filtered light wave and extract polarization information, such as angle and degree of linear polarization, using standard digital image processing algorithms. Although this is the most prevalent sensory approach toward polarization imaging today, the reduction of frame rate by a factor of three and inaccuracy of extracted polarization information due to motion in the scene are major shortcomings.

Monolithic integration of micropolarization filters with CMOS imaging sensors is currently a subject of intense research [7]-[12]. These sensors, known as division of focal plane polarimeters, include silicon photodetectors and micropolarization filters on the same substrate, where the incoming light wave is filtered with spatially distributed micropolarization filters over neighborhoods of pixels. The amplitude of the filtered light wave is recorded by the underlying photodetectors and polarization parameters are computed based only on measured intensity information. Incorporating pixel-pitch-matched polarization filters at the focal plane for visible spectrum has been explored with birefringent materials [7] and thin film polarizers [12]. However, the small imaging array size [9], large pixel size [8]

and small extinction ratios [12] have limited the applications for these polarimeters

In this paper we present a novel polarization image sensor that circumvents the above shortcomings by synergistically combining CCD imaging technology with nanotechnology. The integrated polarization image sensor is composed of a one mega pixel CCD imaging sensor monolithically integrated with aluminum nanowire optical filters. The aluminum nanowire polarization filters are fabricated using interference lithography methods [13] and are deposited directly on top of the imaging array. The pixel pitch of the image sensor is 7.4μm, and the improved spatial sampling resolution and noise characteristics of the image sensor allow this image sensor to be used for low contrast imaging applications at 40 frames per second.

#### IMAGE SENSOR OVERVIEW

Block diagram of the complete polarization image sensor is presented in Figure 1.

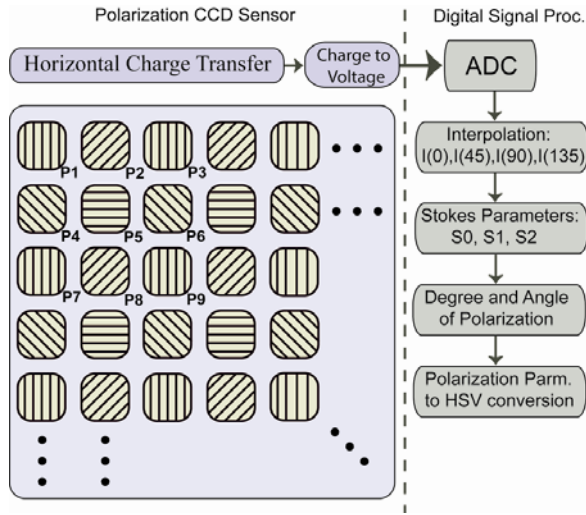


Figure 1. Overview of CCD polarization image sensor.

The sensor is composed of two parts: a charge domain imaging entity and a digital image processing entity. The charge domain imaging entity is composed of an array of 1000 by 1000 buried channel vertical CCDs, 1000 buried channel horizontal CCD register and charge to voltage conversion amplifier. Each pixel is composed of a photodiode and two light shielded buried channel CCDs. The photodiode converts the incident photons into electron-hole pairs and integrates these charges on the intrinsic capacitance of the photodiode. The integrated charge on the photodiode is transferred on the first CCD element in the pixel by activating the transfer gate. The charge from the first CCD is shifted to the second CCD, allowing for a true two phase operation of the CCDs and maximizing the charge transfer efficiency. The charges from the top row of vertical CCDs are shifted in parallel to the horizontal CCDs. The charge from the horizontal CCD register is converted to voltage via a charge amplifier with a conversion gain of 30μV/e<sup>-</sup>. The total well capacity of the photodiode is 20K electrons and the maximum voltage output per pixel is 600mV.

The CCD array of photo elements is covered with an array of pixel-pitch matched nanowire polarization filters. The pattern of the polarization filter array is shown in Figure 1 and it is composed of 4 distinct filters which are offset by 45 degrees. The aluminum nanowires in each filter are 70nm wide, 70nm high and 130nm pitch. The polarization filter array is fabricated by an optimized procedure of interference lithography [13] and deposited directly on top of the image sensor. Since deposition of aluminum on the surface of the image sensor is compatible with standard fabrication procedures of integrated circuits, this fabrication step can be easily integrated during the fabrication of the image sensor at the foundry. The extinction ratio of the polarization filter is determined by the size of the nanowires. In order to achieve extinction ratio of 20 or above, the width of the nanowires must be at least 1/5th of the smallest operational wavelength, i.e. 80nm in order to filter blue light at 400nm [13].

The raw polarization image information is digitized and presented to a digital processing unit for further image processing. The first step in the digital signal processing is interpolation. The raw image data is composed of 1 million data points, from which ¼ is from pixels with 0 degree polarization filter, ¼ is from pixels with 45 degree polarization filter and so on. In order to increase the accuracy of the polarization information, a two point nearest neighbor interpolation scheme is implemented. Hence, the output from the interpolation routine are four image arrays composed of 1 million data points corresponding to the 0°, 45°, 90°, and 135° filtered pixel values.

For example, pixel P2, P4 and P5 records the intensity of the incoming light wave after 45°, 135° and 90° polarization filter respectively. In these three pixels, 0° polarization information from the incident light is not present. The interpolation algorithms can be used to estimate the 0° polarization information for these three pixels. After the interpolation procedure is performed, the new values for these pixels are estimated using equations (1) thorough (3):

$$P2_{0^\circ} = (P1 + P3) / 2 \quad (1)$$

$$P4_{0^\circ} = (P1 + P7) / 2 \quad (2)$$

$$P5_{0^\circ} = (P1 + P9) / 2 \quad (3)$$

where P1, P3, P7 and P9 are the intensity value of the corresponding pixels with 0° polarization filter. Similar interpolation equations are used to estimate the 45°, 90° and 135° arrays.

The first three Stokes parameters are computed on the interpolated data followed by computation of angle and degree of linear polarization. The final step in the digital image processing is to convert intensity, DoLP and AoP into a single composite image. A false color image is produced by mapping the AoP to the hue, DoLP to the saturation of color and intensity, i.e. S<sub>0</sub> parameter, to the value parameter. The false color representation allows for intensity information to be presented as a grayscale image and polarization information to be presented in color. Each angle of polarization is presented as a different color, where orthogonal angles are presented in

opponent colors. The saturation of the color is dictated by the DoP.

## MEASUREMENTS AND RESULTS

We characterized the CCD polarization imaging sensor for responsivity, accuracy of the measured degree and angle of polarization and extinction ratios. The imaging sensor is tested with a uniform and collimated light, where the degree and angle of linear polarization of the incident light is controlled via a computer.

The optical performance of the imaging sensor is evaluated at  $625\text{nm}\pm 5\text{nm}$ ,  $515\pm 5\text{nm}$  and  $460\pm 5\text{nm}$ . A 4" integrating sphere with three ports is used to produce uniform light intensity. Two arrays of narrow band and high intensity LEDs are used as inputs to the integrating sphere. A  $100\mu\text{m}$  pinhole is placed at the output port of the integrating sphere and a 40mm condensing lens is used to produce collimated light. The imaging sensor is placed on a computer controlled rotating stage and is rotated between  $0^\circ$  and  $30^\circ$  in increments of  $2^\circ$ . Hence, the incident angle of the incoming light to the surface of the imaging sensor is varied in a systematic manner. For every incident angle, the angle of polarization of the incident light is swept from  $0^\circ$  to  $180^\circ$  in increments of  $1^\circ$  via computer controlled linear polarization filter. The degree of polarization of the incident light is modulated via a computer controlled variable liquid crystal phase retarder between 0 (unpolarized light) to 1 (linearly polarized light) in increments of  $\sim 0.1$ . The reference angle and degree of linear polarization is obtained with a single calibrated photodetector and mechanically rotating linear polarization filter.

Figure 2 illustrates the responsivity of four neighboring pixels with different polarization filters as a function of the polarization angle of the incident linearly polarized light. All four pixels follow Malus' law for polarization irradiance and are offset by  $45^\circ$  due to the physical orientations of the aluminum nanowires. Hence, the maximum and minimum transmissions between two neighboring pixels are shifted by

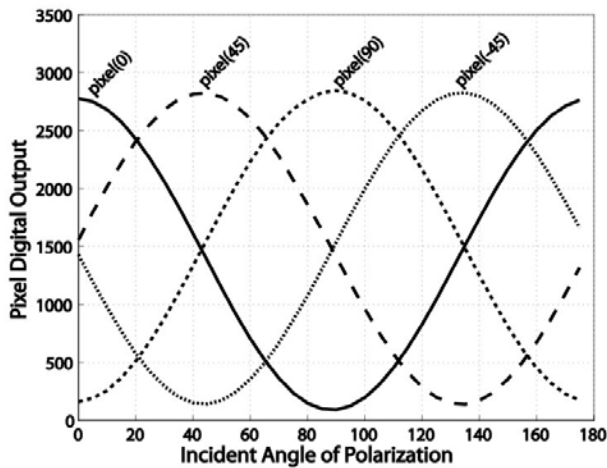


Figure 2: Intensity response of four neighboring pixels as a function of different angles of linearly polarized light. The four pixels have nanowire polarization filters offset by  $45^\circ$  relative to each other.

$45^\circ$ . The maximum transmission for the polarization pixels occurs when parallel polarized light illuminates the photodiode and corresponds to 64% of the total incident intensity. The minimum transmission is 1.1% of the total incident intensity and is recorded when cross polarized light illuminates the photodetector.

Figure 3 depicts the computed angle of linear polarization, as a function of the polarization properties of an incident reference light wave. The angle of linear polarization is computed across the entire imaging array on a neighborhood of 2 by 2 pixels, and the mean values as well as its standard deviations are presented. The linear fit error for the computed angle of linear polarization is 0.2%. The root-mean-square value of the standard deviations for each angle of linear polarization computed on all pixels across the imaging array is  $0.08^\circ$ .

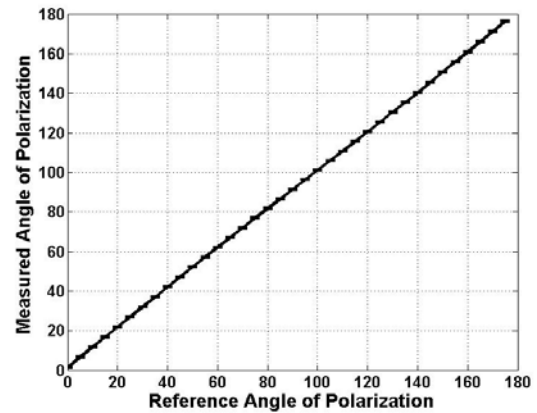


Figure 3: Measured angle of linear polarization from a neighborhood of four pixels as a function of different angles of linearly polarized light

Figure 4 presents the measured extinction ratios as a function of the incident angle of the reference light wave on the surface of the imaging sensor. The incident angle of the impinging light wave is swept between  $0^\circ$  and  $30^\circ$  in increments of  $2^\circ$ . For incident light ( $625\pm 5\text{nm}$  wavelength) perpendicular to the surface of the imaging sensor, the extinction ratios are maximum and equal to 58. The extinction ratio remains constant as the incident angle of the

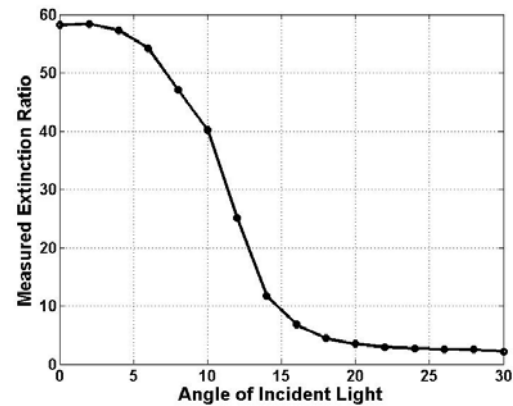


Figure 4: Measured angle of linear polarization from a neighborhood of four pixels as a function of different angles of linearly polarized light

light wave is increased to  $5^\circ$  and rapidly decreases for higher incident angles. For incident angles greater than  $\sim 20^\circ$ , the polarization information is completely lost due to the pixel crosstalk.

Sample images recorded from the polarization CCD imaging sensor are presented in Figure 5. The imaged scene is composed of six linear polarization filters offset by  $30^\circ$  and a black plastic horse figure against a white background. The intensity variations along the plastic figure are minimal and the shape of the figure is difficult to determine in the intensity image presented in Figure 5-a.

The degree of linear polarization image is presented in Figure 5-b, where bright and dark values indicate high and low degrees of linear polarization in the scene respectively. The linear polarization filters have high degree of polarization due to the intrinsic properties of the filters. Figure 5-c presents the angle of linear polarization of the imaged scene. The angles of polarization for the six linear polarization filters are presented in different colors offset by  $30^\circ$ . The angle and degree of linear polarization along the plastic figure exhibit smooth variations due to the curvature of the figure, i.e. surface normal and intrinsic properties of the object, i.e. index of refraction of the object. This sensor captures intrinsic information about the imaged environment, i.e. surface curvature and index of refraction, represented in polarization data space in high resolution and in real-time.

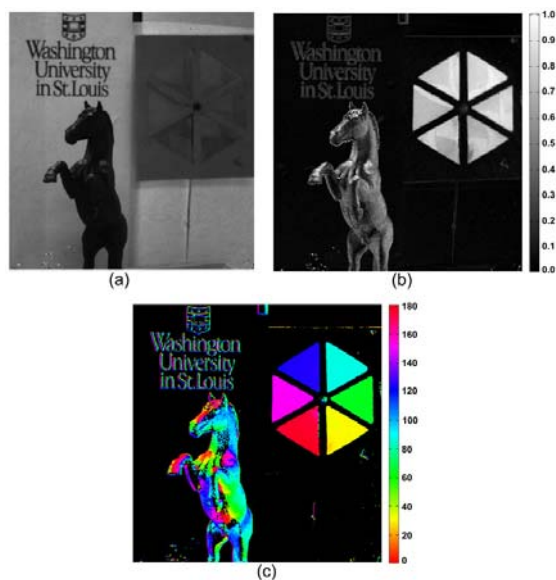


Figure 5: Sample images from CCD polarization imaging sensor of sample objects and linear polarization filters. (a) intensity information; (b) degree of linear polarization and (c) angle of linear polarization of the imaged scene

The polarization imaging sensor is used for real-time 3-D shape reconstruction of moving targets using a single camera view. The degree of polarization captured by the CCD polarization imaging sensor is directly related to the incident angle of the incoming light and the surface normal of the imaged object. The polarization measurements from the

imaging sensor at every frame are converted to surface normal. In Figure 5 the 3-D shape reconstruction of a plastic figure is presented. The degree of polarization image presented in Figure 5-b yields an accurate estimate of the surface profile of the plastic toy and is presented in Figure 5-a.

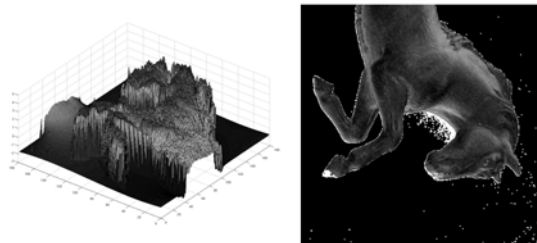


Figure 5-a: Surface normal reconstruction using degree of polarization measurement from the CCD polarization imaging sensor. Figure 5-b: Degree of polarization measurement from the CCD polarization imaging sensor.

## CONCLUSION

We present an integrated polarization sensor capable of computing angle, degree of linear polarization and intensity information at 40fps and consuming 300mW of power. The measured signal-to-noise ratio of the polarization imaging sensor is 45dB and the dynamic range is 65dB. The polarization filters with extinction ratios of 58 can be used for real-time shape reconstruction of objects.

## REFERENCES

- [1] Fossum, E. R., "CMOS image sensors: electronic camera-on-a-chip," *IEEE Trans. Electron Devices* **44**, 1689-1698 (1997).
- [2] Goldstein, D., "Polarized Light," (Marcel Dekker: New York, NY, 2003).
- [3] Schwartz, S.; Namer, E.; Schechner, Y., "Blind Haze Separation," *Proc. IEEE Comp. Vision and Pat. Recog.* **2**, 1984-1991 (2006).
- [4] Treibitz, T.; Schechner, Y., "Active polarization descattering," *IEEE Trans. Pattern Anal. Mach. Intel.* **31**, 385 (2009).
- [5] Lin, S.; Yemelyanov, K.; Pugh, E.; Engheta, N. "Polarization-based and specular-reflection-based noncontact latent fingerprint imaging and lifting," *J. Opt. Soc. Am. A* **23**, 2137-2152 (2006).
- [6] Tyo, J. S.; Goldstein, D. L.; Chenault, D. B.; Shaw, J. A., "A Review of Passive Imaging Polarimetry for Remote Sensing Applications," *Appl. Opt.* **45**, 5453-5469 (2006).
- [7] Andreou, A.; Kalayjian, Z., "Polarization imaging: principles and integrated polarimeters," *IEEE Sensors J.* **2**, 566-576 (2002).
- [8] Momeni, M.I Titus A., "An analog VLSI chip emulating polarization vision of octopus retina," *IEEE Trans. Neural Netw.* **17**, 222-232 (2006).
- [9] Tokuda, T.; Sato, S.; Yamada, H.; Sasagawa, K.; Ohta, J., "Polarisation-analysing CMOS photosensor with monolithically embedded wire grid polarizer," *IEE Electronics Lett.* **45**, 228-230 (2009).
- [10] Zhao, X.; Boussaid, F.; Bermak, A.; Chigrinov, V.G., "Thin Photo-Patterned Micropolarizer Array for CMOS Image Sensors," *IEEE Photon. Technol. Lett.* **21**, 805-807 (2009).
- [11] Gruev, B.; Perkins, R.; York, T., "CCD polarization imaging sensor with aluminum nanowire optical filters," *Optics Express* **18**, pp. 19087-19094 (2010).
- [12] Gruev, V.; Van der Spiegel, J.; Engheta, N., "Dual-tier thin film polymer polarization imaging sensor," *Optics Express* **18**, 19292-19303 (2010).
- [13] Gruev, V.; Van der Spiegel, J.; Engheta, N., "Nano-wire Dual Layer Polarization Filter," *Proc. IEEE ISCAS*, (2009).